

CURRENT PROBLEMS
OF DEVELOPMENTAL BIOLOGY

Mathematical Model of Auxin Distribution in the Plant Root

V. A. Likhoshvai^{a,b}, N. A. Omel'yanchuk^a, V. V. Mironova^a, S. I. Fadeev^{b,c},
E. D. Mjolsness^d, and N. A. Kolchanov^{a,b}

^a Institute of Cytology and Genetics, Siberian Branch of the Russian Academy of Sciences,
prosp. Acad. Lavrent'eva 10, Novosibirsk, 630090 Russia

^b Novosibirsk State University, ul. Pirogova 2, Novosibirsk, 630090 Russia

^c Institute of Mathematics, Siberian Branch of the Russian Academy of Sciences,
ul. Koptyuga 4, Novosibirsk, 630090 Russia

^d Institute of Genomics and Bioinformatics, University of California, Irvine, CA 92607 USA

E-mail: likho@bionet.nsc.ru

Received May 29, 2007

Abstract—Auxin regulation of plant growth and development is mediated by controlled distribution of this hormone and dose-dependent mechanisms of its action. A mathematical model is proposed, which describes auxin distribution in the cell array along the root longitudinal axis in *Arabidopsis thaliana*. The model qualitatively simulates auxin distribution over the longitudinal axis in intact roots, changes in this distribution at decreased auxin transport rates, and restoration of the auxin distribution pattern with subsequent establishment of new root meristem in the course of root regeneration after the ablation of its tip. The model shows the presence of different auxin distribution patterns over the longitudinal root axis and suggests possible scenarios for root growth and lateral root formation. Biological interpretation of different regimes of model behavior is presented.

DOI: 10.1134/S1062360407060057

Key words: *Arabidopsis thaliana*, development of plant root, auxin transport, mathematical model.

Natural auxin (indoleacetic acid, IAA) is a unique substance involved in the regulation of various biological processes. In *Escherichia coli*, auxin activates different protective mechanisms underlying the resistance against stresses (Bianco et al., 2006). Some soil bacteria synthesize auxin for interaction with their host plants (Costacurta and Vanderleyden, 1995). In *Saccharomyces cerevisiae*, IAA regulates cell growth and differentiation inhibiting yeast growth at high concentrations and inducing differentiation into an invasive form at low concentrations (Prusty et al., 2004).

In the plant world, the regulatory mechanisms involving auxin were complicated in the course of evolution: from simple relationships in lower plants to complex mechanisms of auxin distribution and auxin-mediated regulation in higher plants (Cooke et al., 2002). In the root of higher plants, the highest auxin concentration was recorded in the meristem (Sabatini et al., 1999) and in cells of the root cap initials and quiescent center (Fig. 1). The location of auxin maximum remains practically unchanged during the entire life of a plant despite continuous cell divisions in the meristem.

The distribution of auxin depends on its biosynthesis, inactivation (conjugation and direct oxidation), diffusion, and active transport (Woodward and Bartel, 2005). Nevertheless, a significant part of auxin present in the root is synthesized in the above-ground part of the

root until the stage of lateral roots formation (7–8 days after germination) and is transported to the root via the vascular tissue (Ljung et al., 2005). Active cellular auxin efflux plays the main role in distribution of auxin in the root also until this time (Friml et al., 2003; Petrasek et al., 2006). There are three main classes of auxin transporters in *Arabidopsis thaliana*: AUX, PGP, and PIN, which provide its direct influx or efflux from the cell (Kramer and Bennet, 2006). In the vascular tissue, PGP1 and PIN1 are localized on the basal side of cells (Blilou et al., 2005; Geiser and Murphy, 2006), while AUX1 provides for auxin influx in the cell on the apical side of phloem cells (Swarup et al., 2001).

It has been shown experimentally that auxin is capable of both activating and inhibiting its active transport. Degradation of proteins AUX/IAA, which repress transcriptional factors of ARF family, is regulated by auxin (Dharmasiri and Estelle, 2004). These factors activate expression of many genes, including transporter gene *PIN1*, after releasing from inhibition (Sauer et al., 2006). Proteins of PIN family circulate continuously between the plasma membrane and endosomes (Geldner et al., 2001; Paciorek et al., 2005). Auxin inhibits endocytosis and thereby increases the amount of these proteins on the membrane and, hence, its own transport from the cell. Degradation of PIN proteins takes place at high auxin concentrations (Vieten et al., 2005) and,

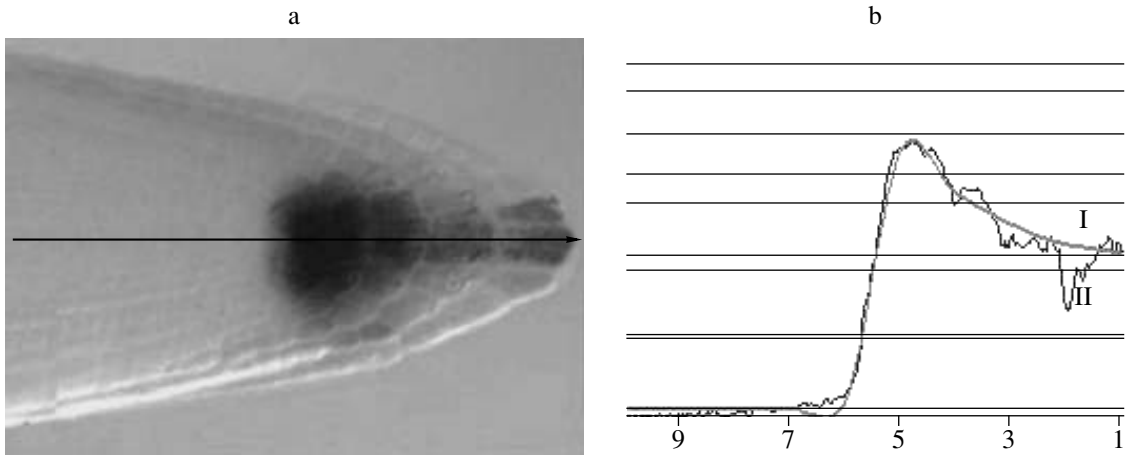


Fig. 1. Auxin distribution in the root: (a) in the root tip, (b) along the central axial zone of root cells. (a,I) from Wang et al., 2005, (a, II) calculated according to the model—formula (1).

as a result, the auxin efflux from the cell decreases (Sieberer et al., 2000).

Thus, key components of auxin transport regulation in the root of *A. thaliana* early seedling, their interactions, and roles have been defined.

Here, we present a one-dimensional mathematical model describing qualitative auxin distribution in the cells on the central axis of *A. thaliana* root, and auxin distribution under the conditions of slower active transport (for example, when the root is treated with an inhibitor of the polar auxin transport), and restoration of qualitative auxin distribution and, hence, meristem restoration in the root during its regeneration after root tip ablation.

MATERIALS AND METHODS

Processing of experimental data. Experimental data are presented as photographs of sections of the plant roots, in which the pattern of auxin distribution was determined using transgenic constructs DR5:GUS or DR5:GFP (Sabatini et al., 1999; Wang et al., 2005). We scanned these photographs using ImageJ software (http://www.rsmas.miami.edu/personal/cparis/pvnfor/doc/imagej/using_ij.pdf) and thereby translated the experimental data into the relative quantitative ones.

Model description. The distribution of auxin is considered in a file of *n* cells along the central root axis, where the most distal cell located in the root tip is the first. According to the anatomy data, such file of cells will include successively three cells of the root cap (sloughed cells are not taken into account), cells of initials of the root cap, quiescent center, and vascular tissue, one from each, differentiating cells of the vascular tissue, and differentiating cells of vascular bundles (Dolan et al., 1993; Benfey and Sheres, 2000). A cell of the zone of shoot-root transition or a cell of the vascular

tissue may be the last cell in the file. The flow of auxin from cell *n* towards cell 1 is considered. Auxin concentration in each of *n* cells is calculated in the model with an account of the following processes:

(1) Auxin may diffuse passively from cell to cell.

(2) It may be transported by means of facilitator proteins and the rate of active transport depends on auxin concentration: it is high at low concentrations and low at high concentrations (Sieberer et al., 2000; Geldner et al., 2001; Paciorek et al., 2005; Vieten et al., 2005; Sauer et al., 2006).

(3) A special boundary condition is used for the first cell of the model: auxin may be transported from it only into the second cell and only by dissipation.

(4) Auxin dissipation is also considered, which includes the processes leading to its decreased concentration in the cell, such as conjugation, direct oxidation, or horizontal active transport (into the cells not considered in the model).

Auxin biosynthesis in the root, as well as active transport in other direction and cell specialization are not considered in the model. Taking into account the above said, we proposed the following model for calculation of auxin distribution in the root:

$$\begin{aligned}
 \frac{da_n}{dt} &= \alpha + P_t a_{n-1} - P_i a_n - K_d a_n - K_0 a_n f(a_n), \\
 \frac{da_i}{dt} &= P_t (a_{i+1} + a_{i-1}) + K_0 a_{i+1} f(a_{i+1}) \\
 &\quad - 2P_t a_i - K_d a_i - K_0 a_i f(a_i), \quad i = \overline{n-1, 2}, \\
 \frac{da_1}{dt} &= -P_t a_1 - K_d a_1 + P_t a_2 + K_0 a_2 f(a_2),
 \end{aligned}
 \tag{1}$$

where *n* is the number of cells in the model, *a_i* is auxin concentration in cell *i*, *K_d* is the coefficient of dissipa-

tion, P_i is the coefficient of passive transport (diffusion) identical in both directions; $K_0 > 0$ has the meaning of the constant of the active transport rate, α is the constant of the intensity of auxin supply to cell n . For description of active transport in formula (1), a generalized Hill function $f(a_i)$ is used:

$$f(a_i) = \left(\frac{\left(\frac{a_i}{q_{11}}\right)^{p_1}}{1 + \left(\frac{a_i}{q_{11}}\right)^{p_1}} \right) \times \left(\frac{1}{1 + \left(\frac{a_i}{q_{12}}\right)^{p_2}} \right), \quad (2)$$

where q_{11} is the constant of threshold of auxin-dependent transport activation, q_{12} is the constant of threshold of saturation of auxin-dependent transport activation, q_2 is the constant of threshold of auxin-dependent transport inhibition. p_1 and p_2 are coefficients of nonlinearity of the mechanisms of activation and inhibition, respectively. The first factor of equation (2) described the mechanism of activation of the auxin transport from the cell and the second described the mechanism of inhibition of the auxin transport by high concentrations. The function behaves qualitatively in the following way: it

is close to zero at low a_i values, increases to a certain maximum at the intermediate values, and decreases from maximum to zero at the high values.

The method of Gear (1971) was used to calculate the time-related evolution of the mathematical model variables (calculation of Cauchy problem). Multiple stationary solutions were investigated using the method of continuation by parameter (Fadeev et al., 1998).

RESULTS

Qualitative correspondence of model solutions to experimental data. The auxin distribution in the root is characterized by the presence of sharp concentration gradient and its decrease from a maximum point (4th–5th cell) to the root tip (Fig. 1).

Stationary distribution of auxin in the root tip calculated from the model at $n = 52$ and set parameters corresponds qualitatively to the experimental data (Fig. 1b). We will use below references to the following model parameters, at which this qualitative adequate auxin distribution is reached.

Parameters	α	P_i	K_d	K_0	q_{11}	q_{12}	q_2	p_1	p_2
Dimension	cu/tu	1/tu	1/tu	1/tu	cu	cu	cu	dl	dl
Value*	1	0.08	0.0045	0.25	1	100	3	2	10

* Given in conditional units: cu, concentration; tu, time; dl, dimensionless value.

Multiple stationary distributions of the model. The model has a significant number of different steady state distributions of auxin concentration at the set parameters and seven of them are presented in Fig. 2. All stationary auxin distributions in the root tip correspond qualitatively to the experimental data (Fig. 1b). Let us introduce a classification of distribution types for simplification. We will designate distribution as a vector (i, j, k). Components i and k designate the presence (1) or absence (0) of a maximum in the root beginning (i) or end (k), j corresponds to the number of internal auxin maxima and assumes integral values from 0 to n . We found four types of distributions. The first distribution type (0, 0, 1) has only one terminal peak and low auxin concentration at the base and middle part of the root. This type of distributions is realized if the root length is set as sufficiently big ($n > 37$) and the cell concentration of auxin as low. The second distribution type (1, 0, 1) has a similar maximum auxin concentration at the root tip, but is also characterized by an additional maximum as a descending gradient from the shoot-root junction towards the root end. The distribution is realized from zero initial data, if the root length is sufficiently small. If n is sufficiently high ($n \geq 37$ at the set parameters), the initial data for reaching distribution (1, 0, 1) should also correspond qualitatively to distribution (1, 0, 1). The third and fourth distribution types are (0, j, 1) and

(1, j, 1). They have one or more peaks of auxin distribution in the root middle.

Analysis of dependence of the position of maximum auxin concentration in the root tip from root length. The quiescent center has the same position with reference to the root end in the course of growth (Jiang and Feldman, 2005). In our model, the last cell before the maximum in the root tip corresponds to this position at the set parameters. We carried out a spot check of dependence of the position of auxin maximum in the root tip on root length n . Figure 3 presents final stationary distributions of auxin concentration in 15 terminal root cells obtained for $n = 15, 27, 37, 52, 82,$ and 102 . It can be seen that the maximum position in the root tip depends on the root length at $n \geq 37$ and is stable at $n \leq 27$. This is explained by the formation of distribution (1, 0, 1) short root lengths, which is more stable to n . On the contrary, distribution (0, 0, 1) is formed from zero initial data in long roots. This distribution depends on the root length. However, we found that the distribution obtained from zero Cauchy problem belongs to a family of distributions (0, 0, 1) and there are distributions among the members of this family, in which the 5th cell has the maximum auxin concentration. Since the concentrations are subject to fluctuations, it can be proposed that during the root growth, a family of distributions (0, 0, 1) is realised. The family

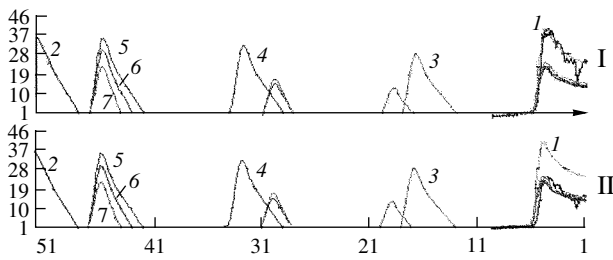


Fig. 2. Examples (1–7) of stable distribution of auxin concentrations along the central root axis from the model solutions. I, results of calculation of Cauchy problem with zero initial data; II, the same with initial data $a_{52} = 35$, $a_{51} = 25$, $a_{50} = 16$, $a_{49} = 8$, $a_{48} - a_6 = 1$, $a_5 = 13$, $a_4 = 12$, $a_3 = 11$, $a_2 = 10$, $a_1 = 9$. Calculations were carried out for the root length over the central axis, $n = 53$.

Here and in Figs. 3, 4, and 6–8: abscissa: ordinal number of the cell (no. 1 corresponds to the terminal cell of the root); ordinate: auxin concentration in the cell, cond. unit.

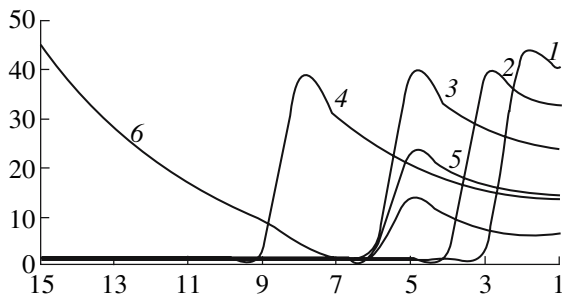


Fig. 3. Stationary auxin distribution obtained with the help of model and set parameters as a result of calculation of a Cauchy problem with zero initial data and $n = 102$ (1), 82 (2), 52 (3), 37 (4), 27 (5), and 15 (6).

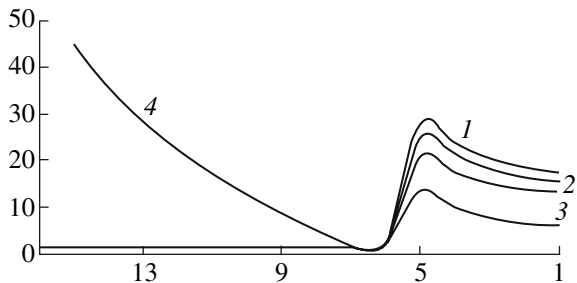


Fig. 4. Stationary auxin distribution obtained by the model with set parameters as a result of calculation of a Cauchy problem with the following initial data: $a_1 = 8$, $a_2 = 9$, $a_3 = 10$, $a_4 = 11$, $a_5 = 12$, $a_6 - a_{n-4} = 1$, $a_{n-3} = 8$, $a_{n-2} = 15$, $a_{n-1} = 25$, $a_n = 35$; $n = 52$ (1), 37 (2), 27 (3), and 15 (4).

might be more stable to the root length than a single distribution.

Unlike distribution (0, 0, 1), distribution (1, 0, 1) proved to be more stable to changes in the root length in a computational experiment at the set parameters: the terminal maximum fell to the 5th cell irrespective of the

root length (Fig. 4). The data obtained suggest that the model reproduces the phenomenon of dynamic equilibrium of auxin distribution in the tip of a growing root, which does not depend on the type of stationary distribution, but different distributions demonstrate different stability of the position of a concentration maximum. The peak position is most stable in distributions (1, 0, 1) and (1, j, 1) and less stable in distribution (0, 0, 1). All these characterized families of distributions have at least one solution best corresponding to the experimental data.

Dependence of stationary distributions from fluctuations of auxin concentrations in the cells. We performed a computational analysis of stability of different distribution types with reference to fluctuations of auxin concentration in the cells at $n = 52$ and set parameters based on the following type experiment. We changed auxin concentration in a stationary distribution of a certain type in a certain cell or group of cells and then solved the Cauchy problem taking the obtained perturbed distribution of auxin concentration as the initial data. As a result, a new distribution was formed. In one calculation, we fixed the type of initial distribution, character of fluctuation (ordinal number of cell, where fluctuation takes place, and value of fluctuation expressed as a defined auxin concentration), and type of terminal distribution.

Perturbation of distribution (0, 0, 1). After imposed increased auxin concentration in an indexed cell, pattern (0, 0, 1) is not changed if this concentration is below ~ 4 cu and evolves into patterns (1, 0, 1) or (0, 1, 1) at concentrations above this level. So, auxin concentration of ~ 4 cu is a transition threshold of (0, 0, 1) for (1, 0, 1) or (0, 1, 1). At concentrations below the threshold one, the initial distribution is not changed, while at concentrations above the threshold one, a new type of stationary distribution is formed. A single fluctuation with a rather small change of concentration induces the formation of a one-cell-wide peak. The increase of fluctuation value over 10-fold threshold value leads to the peak smearing (widening over several cells and shortening).

If a fluctuation is imposed in the indexed cell closest to the stem (no. 52 at $a_i > 4$ cu and no. 51 at $a_i > 454$ cu) or inner root cells (no. 51–8), distributions (1, 0, 1) or (0, j, 1), respectively, are formed. Additional auxin maxima in the final stationary distributions (0, 1, 1 and (1, 0, 1) are positioned in the same cells, where initial fluctuations took place, but auxin concentration in these maxima changed up to 11–17 cu, irrespective of the initial fluctuation value.

Formation of distribution (0, 0, 1). Transition from distributions (1, 0, 1) or (0, j, 1) to (0, 0, 1) is realized at a decrease of auxin concentration in maximum points below the threshold value (< 4 cu). If we take into account that auxin concentration in these maxima equals to 11–17 cu, this transition is less probable than the inverse one, since it requires a stronger fluctuation.

This transition may be facilitated in vivo by redistribution of auxin to the lateral cells, which are not considered in the model.

Formation of distribution (1, j, 1). Transition from distribution (0, j, 1) to (1, j, 1) is realized similarly that from (0, 0, 1) to (1, 0, 1); note that transition from (1, 0, 1) requires stronger fluctuations ($a_i > 25$ cu). Therefore, the probability of such transition will be lower than from (1, 0, 1) to (0, 0, 1). By analogy, transition from (1, j, 1) to (0, 0, 1) is preferentially realized via (1, 0, 1), since the value of fluctuation for such transition will be minimal. In addition to the above said, direct and inverse transitions from (0, j, 1) to (1, 0, 1) without intermediate transitions to (0, 0, 1) or (1, j, 1) are impossible in computational experiments. The summary data on probabilities of transitions between different distribution types obtained in computational experiments allows us to plot a scheme for rotation of auxin distribution patterns in the root (Fig. 5).

Formation of internal peaks in distribution (0, j, 1). We expected that internal maxima in distribution (0, j, 1) might provide positional readouts for lateral root formation. To estimate the influence of auxin fluctuations on the number of internal maxima and other features of this auxin pattern, we imposed fluctuations one by one in different positions along the root main axis. It turned out that the number of peaks in stationary distribution was limited and depended on the value of fluctuations. If the formation of one peak in the entire region of cells no. 51–8 is equiprobable at weak fluctuations, the formation of next peaks requires a stronger fluctuation applied at a certain distance from the first peak. Otherwise, if fluctuation takes place between the shoot-root junction and internal maximum in distribution (0, 1, 1), the initial maximum will disappear and a new maximum will appear in the point of fluctuation and if fluctuation will appear between internal maximum and root tip, this will not change the initial distribution. The maximum number of peaks observed in this simulation equaled six at $n = 52$ and 14 cu fluctuations, and the distance between the positions of fluctuations of no less than seven cells. The auxin concentration in cells within regions of its maximum was higher in cells located closer to the root tip, thus corresponding to the experimental data about the appearance of lateral roots in the basal root part. The model shows also that the formation of internal auxin maxima in the root is determined to a great extent by the total auxin distribution, rather by the local auxin concentration in the cell.

Influence of fluctuations on auxin distribution estimated at other sets of parameters. Varying individual parameters led in most cases to the same solutions. Adequate sets of parameter values enabling the desirable model behavior were parameter sets, for which the model solutions reproduce the experimental data. However, it was not the case for varying parameter p_2 , which determines the degree of nonlinearity of the active transport repression. At $p_2 = 5$, the model exhibits buff-

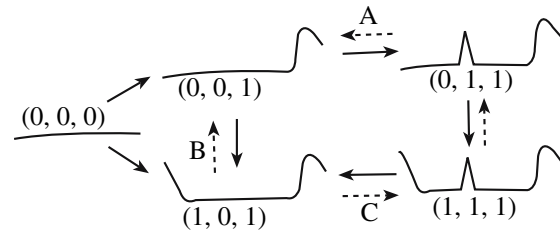


Fig. 5. Succession of type of auxin distributions in the model. Solid line—more probable transition, dotted line—less probable transition.

ering against local changes of the root concentration of auxin. For example, the increase of auxin level in tens of times in cells 11 to 52, did not induce visible changes in stationary auxin distribution. Only the fluctuations that exceed 60 cu led to an insignificant shift of terminal auxin maximum towards the shoot by no more than 12 cells irrespective of the increased fluctuation value. Thus, no distributions (1, 0, 1) and (0, j, 1) were observed in model (1) at $p_2 = 5$, while distribution (0, 0, 1) was predominant.

Dependence of the model from variation of parameters. The set of parameters fitting to the experimental data is not unique. Varying parameters within sufficiently wide limits also provides solutions qualitatively corresponding to the curves of auxin distribution in the root in vivo. Since the available experimental data do not allow a more precise estimation of the model parameters, we evaluated of the model's sensitivity to variation in individual parameters. This was important also because the biologically realistic range for parameters can be wide enough due to probable conservation of the studied process among plant species.

Influence of auxin flow from the shoot to the root (α) on auxin distribution. The intensity of auxin flow from the shoot to the root is a parameter of our model, which can undergo significant changes in time, and hence, its influence on stationary auxin distribution was studied in computational experiments with the model. Calculations were carried for $\alpha = 1$ –1.6 with a step of 0.1 and the calculation for the next ascending parameter α was based on the Cauchy problem solutions, in which the stationary distribution from the preceding calculation was taken as an initial value. The zero initial data were taken for the first calculation. Such series of stationary distribution gives an idea about the dynamics of auxin distribution in the root as its flow from the shoot to the root increases (Fig. 6).

It can be seen from calculations that the increase in the rate of auxin flow from 1 to 1.4 does not increase the type of distribution (0, 0, 1) to another, but the position of a maximum is shifted inside the root, but no farther than 6th cell from the root tip, while the increase in the flow intensity from 1.4 to 1.5 leads to the appearance of an internal peak in the 15th cell. The terminal peak

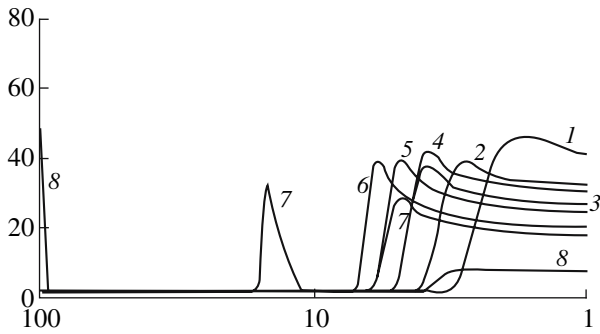


Fig. 6. Stationary auxin distributions realized in the model at set parameters and different α values. Distributions are obtained as a result of calculation of the Cauchy problem with zero initial data (1) and with stationary distributions from the preceding calculations (2–8). $\alpha = 1$ (1), 1.1 (2), 1.2 (3), 1.3(4), 1.35 (5), 1.4 (6), 1.5 (7), and 1.6 (8).

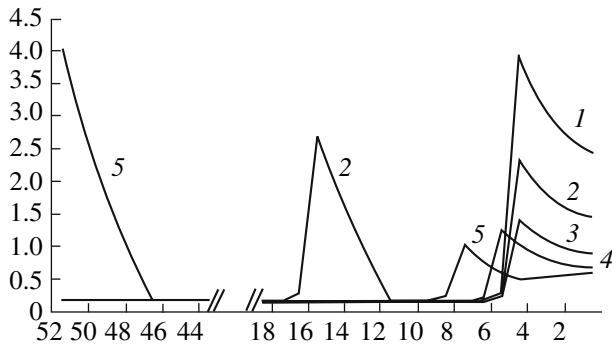


Fig. 7. Changes of auxin distribution after decrease of parameter k_0 equal to: 1, 0.25; 2, 0.2; 3, 0.15, 4, 0.13, and 5, 0.1.

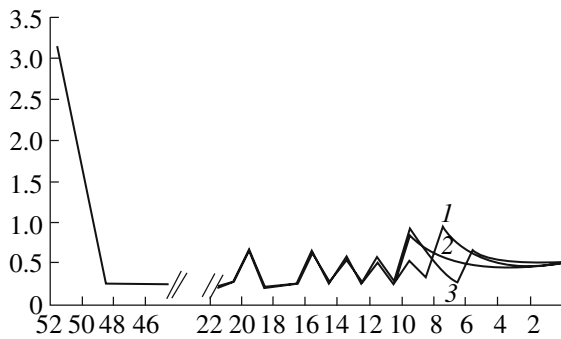


Fig. 8. Unstable fluctuations of auxin concentrations at $k_0 = 0.08$. Distributions 1–3 have been obtained with a difference of 1000 tu.

returns to the 5th cell (Fig. 6; 6 and 7) and the next level of intensity $\alpha = 1.6$ already forms distribution (1, 0, 1).

Influence of coefficients of the rate of active transport on auxin distribution in the root. The active auxin

transport is written in the model as a generalized Hill function and its value is determined by several parameters. They include, above all, the constant of active transport rate k_0 , which determines linear changes in the active transport rate, and constant of the threshold of auxin-dependent transport inhibition q_2 .

At the above set of parameters, zero initial data, and $n = 52$, a decrease of parameter k_0 from 0.25 to 0.10 cu does not change the position of auxin maximum in the root tip, but decreases the maximum level. Distribution (0, 0, 1) is observed in the area of k_0 values from 0.25 to 0.2. At $k_0 = 0.2$, an additional internal auxin maximum appeared, as a result of which distribution (0, 1, 1) is formed instead of (0, 0, 1). Distribution (0, 0, 1) is preserved until $k_0 = 0.15$, where distribution (0, 0, 1) is again restored. At $k_0 = 0.10$, distribution (1, 0, 1) is formed (Fig. 7), which is rather rapidly, already at $k_0 \leq 0.08$ is substituted for a qualitatively new type of stationary distribution as undamped oscillations. Fluctuations with significant amplitudes are observed in a sufficiently narrow zone of cells (3rd to 10th) in the root tip, while fluctuations of concentrations in other cells are so weak that look as stable distributions with several maxim in the root middle (10th to 20th cell) (Fig. 8).

A somewhat different pattern of changes was observed at a decreased k_0 , if distributions (0, 0, 1) or (1, 0, 1) were used as initial data. Such conditions allow simulation of auxin distribution in the root before lateral root initiation: intermediate distribution (0, 1, 1) is not formed, while a maximum in the root tip is localized precisely in the 7th cell.

Note that at $p_2 = 5$ or $k_d = 0.45$ (all other parameters were hold fixed), the smearing of the terminal maximum of auxin concentration was observed: it was shifted towards the shoot and decreased auxin level. Thus, at such parameters, the results of computational experiment reproduce the experimental data on inhibition of active transport by 1-N-naphthylphthalamic acid: a two-fold decrease of active transport leads erosion of the maximum auxin concentration (Sabatini et al., 1999; Wang et al., 2005).

Analysis of auxin distribution at a lower q_2 value has shown a picture similar to that in the case of k_0 changes. There was also successive formation of distributions (0, 0, 1), (0, 1, 1), (0, 0, 1), and (1, 0, 1) from the initial zero data. However, distribution (1, 0, 1) was observed within rather wide limits of the parameter variation ($1.35 q_2 < 2.75$), thus suggesting that this distribution is preferential at a low threshold of auxin transport inhibition. At $q_2 < 1.35$, undamped chaotic fluctuations with small amplitude occurred in cells nos. 3–12. Similarity of the system behavior from parameters k_0 and q_2 with the experimental data becomes understandable from formula (2): the rate of active auxin transport was decreased in both computational experiments, which ensured qualitatively identical results.

Influence of the degree of nonlinearity of the mechanism underlying active transport on the model behav-

ior. In addition to the coefficients that determined the active transport rate, the parameters of nonlinearity of the mechanism underlying activation/repression of auxin transport from formula (2) $o_1 = 2$ and $p_2 = 10$ are no less important. The value of p_1 is fixed on the basis of biological data suggesting that activation is realized by way of increased efficiency of transcription. It has been shown that transcriptional factors of the family ARF ensuring the primary response to auxin form dimers at the conservative binding site AuxRE, widely represented in the *A. thaliana* genome (Ulmasov et al., 1999). Transcription of proteins of the family PIN is realized via this regulatory mechanism (Sauer et al., 2006). There are no available data for parameter o_2 : repression is realized via proteasome-dependent degradation of transporter proteins of the PIN family with many intermediate stages and involved substances. It is obvious that down regulation of active transport might be very effective when auxin concentration reaches the inhibition threshold, so we specified high p_2 value. The influence of the degree of nonlinearity of the mechanism underlying active transport on auxin distribution was studied in more detail.

Simulation shows that when p_1 decreases from 2 to 1, self-triggering of actin fluctuations in the cells takes place, which at $p_1 = 1$ (corresponds to monomeric transcriptional factors) and other parameters holding is preserved even at very high p_1 values (> 50). Auxin distributions are adequate to the experimental data at $p_1 = 2$ or 3. An increase in the degree of nonlinearity up to $p_1 = 4$ leads to a stationary auxin distribution with a maximum in the 3rd cell and at $p_1 \geq 5$ in the last cell. Simultaneous increase of p_2 slightly affects the type of distribution at the set parameters. A qualitative adequate auxin distribution at altered p_1 may be obtained if parameter q_{11} undergoes simultaneous changes. For example, a good correspondence with the experimental data was obtained at ($p_1 = 1, q_{11} = 0.1$) or ($p_1 = 5, q_{11} = 1.5$) and holding other parameters fixed. We considered also the influence of parameter p_2 on the behavior of our model.

It is evident that an increase of this parameter enhances autoinhibition of active transport when a threshold value of auxin concentration is reached. The results of calculations (data not published) suggest that the model behavior undergoes slight change at successive values $p_2 = 10, 20,$ and 50 . Thus, nonlinearity is actually a factor of the model adequate behavior (formula (1)). Determination of the lower boundary of parameter p_2 , when the correspondence of the model (formula (1) to the experimental data is still possible, is of real interest. A deeper biological interpretation of the processes underlying the mechanism of autoinhibition and described in the model by generalized Hill function will bring further decrease in the degree of nonlinearity.

DISCUSSION

Here we suggest, using computer simulations that polar active auxin transport, as well as the terminal cell presence suffice to confer experimentally observed auxin distribution in the root to be formed. The following model components are responsible for this target model:

- (1) Autoactivation of auxin transport from an indexed cell towards the root tip by low auxin doses;
- (2) autoinhibition of the own active transport by high auxin doses;
- (3) presence of acropetal auxin flow from the shoot to the root, and
- (4) presence of a boundary condition—last root cell, from which auxin may move only to the preceding cell by diffusion, as well as dissipate.

Desired auxin distributions along the central root axis are formed as a result of interaction of the above factors at certain ratios of parameters. Parameters specify the rates of passive and active transport, as well as those of degradation and intensity of auxin flow from the shoot to the root. There is no need to use other mechanisms or take into account cell specialization to obtain qualitative coincidence of the model calculation to the experimental data (Fig. 1).

It follows from the model that active polar transport system has a rather narrow range of activity at low auxin concentrations. Such transport system is realized in the root vascular tissue, in which auxin is actively transported from the shoot to the root tip cells (acropetal transport). As a result, auxin is accumulated in the root tip cells and its concentration increases and, therefore, the system of polar active transport is switched off and passive auxin efflux from the cells in the inverse direction (from the root tip towards its base) takes place. The final position of auxin maximum in the model is determined by the balance of oppositely directed flows between the zones of active and passive transport. Let us remember that our model considers only PIN1-regulated auxin transport, which makes the greatest contribution to the acropetal auxin transfer from the shoot to the root in the early seedling (Friml et al., 2003; Ljung et al., 2005). PIN1 is expressed in the root vascular tissue and its weak expression is sometimes observed in the quiescent center (Blilou et al., 2005; Geisler and Murphy, 2006). The domain of PIN1 expression in the root and asymmetrical localization of this protein in the cell agree with the model settings and outputs.

This model reproduces some essential specific features of the auxin-dependent root development. A maximum of auxin concentration in the root tip may be formed in the model from any initial distribution and, hence, simulates the experiments on meristem regeneration and, therewith, restoration of the maximum of auxin concentration after the root ablation (Xu et al., 2006). After the mechanical damage of the root mer-

istem, auxin is still supplied to the distal root cells, where its concentration increases until the beginning of active transport inhibition, as experimentally confirmed by the absence of PIN1 expression in the root tip (Xu et al., 2006). The auxin distribution with a maximum in a layer separated by several cells from the root tip is a result of these processes. This mechanism may serve as a basis for the quiescent center regeneration and its positioning in the root meristem.

The experimentally observed smearing of the zone of high auxin concentrations in the case of suppression of the active transport rate is also inherent in our model. This effect was observed in the experiments on treatment of the *A. thaliana* roots with 1-N-naphthylphthalamic acid, an inhibitor of polar active auxin transport (Sabatini et al., 1999; Wang et al., 2005). This property is realized in the model at certain sets of parameters, for example, if the degree of nonlinearity of the active transport inhibition is low ($p_2 = 5$) or the rate of diffusion is sufficiently high.

Several mechanisms for the formation of lateral roots can also be proposed on the basis of analysis of the model. These mechanisms are based on additional maxima of auxin concentration along the root observed in the model solutions. While redistributing, auxin can enter and accumulate in the pericycle cells, where the initiation of lateral shoots was experimentally shown (Casimiro et al., 2003). The results of experiments (De Smet et al., 2007), in which a local increase of auxin concentration in the protophloem cells at the sites of prospective appearance of lateral root primordia, can serve as an evidence of the influence of auxin from the conducting tissues on the formation of lateral roots. In the model, such effect was observed in the following experiments.

(1) Fluctuations of the initial auxin concentrations in the cells. This mechanism is probable in the case when the above-ground part of a plant develops at a higher rate than the root system. The auxin concentration in some root cells, close to the above-ground part, may exceed the threshold value. Active transport is switched off and, while the root continues to grow, the maximum auxin concentration is maintained in these cells. While redistributing, auxin may be transported from these cells to the pericycle cells and lead to the lateral root appearance.

(2) Undamped fluctuations of auxin concentrations in the root cells at current moments of time. In the case of certain sets of parameters, for example, a low coefficient of active transport, such undamped fluctuations are observed in the model. It can be proposed that this mechanism underlies the formation of lateral roots in some plant species. In this case, the development of lateral roots takes place intensely and irregularly as a result of nonstationary processes of auxin redistribution.

Analysis of the model suggests that different types of distribution of the auxin concentration in the cells

may be realized in different ways and at different stages of root growth. It can also be proposed that local maxima of auxin concentrations with different localization are responsible for different events: in the root region close to shoot the govern its thickening and, possibly, the growth of lateral roots at the root base, and, in the root end, normal functioning of the root meristem. Internal maxima may be responsible for the appearance of lateral root primordia.

One of possible variants of root growth can be proposed. Let the root be short and, in this case, distribution (1, 0, 1) is formed in it. It controls two processes: root elongation and thickening. Thickening will take place the root base, where the auxin concentration is high, and lead to a decreased intensity of the flow, by analogy with a decreased rate of river flow in a wide part. As a result, the maximum will move to the boundary between the root wide and thin parts, where its thickening continues. Successive movement of the peak of auxin concentration along the root will cause root thickening over the entire length and, as a result, the intensity of flow will fall and distribution (1, 0, 1) will be transformed into (0, 0, 1). At this stage, the root elongation will be predominant process. In parallel, distributions (0, j, 1) may be spontaneously formed from (0, 0, 1) as a result of local fluctuations of auxin concentrations in the cells, which will lead to the growth of lateral roots. However, as the plant grows, the intensity of flow to the root at the stage of predominant elongation, rather than thickening, will increase. As a result, a regular phase of the initiation of new lateral roots will take place at a certain stage. While repeating cyclically, the described stages will lead to such dynamics of root growth and predominance of such processes that will respond more adequately to requirements of the organism at each stage of plant development.

The above model is developed on the principle of maximum simplification, which allowed us to propose the most general mechanism reproducing the experimentally observed auxin distribution. We cannot exclude that some properties of the model may be a sequence of its simplicity, but hope that future experiments will reveal which aspects of model solutions (stationary points, oscillations) are biologically relevant.

At present, we do not have enough quantitative data, that will allow us to give preference to certain parameter values in the model and, thereby, narrow the combinatorial diversity of possible solutions. Therefore we analyzed the main properties of the model and types of auxin distribution at different sets of parameter values. It remains still to learn at what sets of parameters, the model reflects the actual data better. It may well be that different sets of parameters will correspond to different plant species, since the processes in question are conservative for the entire plant kingdom.

ACKNOWLEDGMENTS

This study was supported by the Federal Agency of Science and Innovations, state contract no. 02.467.11.1005, Russian Foundation for Basic Research, project nos. 05-07-98011 and 05-07-98012, Russian Academy of Sciences, project no. 10104-34/P-18/155-270/1105-06-001/28/2006-1, Program of the Russian Academy of Sciences Molecular and Cell Biology, Siberian Branch of the Russian Academy of Sciences, integrational project no. 115, and National Science Foundation of the USA, FIBR EF-0330786 "Modeling of Development and Bioinformatics".

REFERENCES

- Benfey, P.N. and Scheres, B., Root Development, *Curr. Biol.*, 2000, vol. 10, no. 22, pp. 813–815.
- Bianco, C., Imperlini, E., Calogero, R., et al., Indole-3-Acetic Acid Regulates the Central Metabolic Pathways in *Escherichia coli*, *Microbiology*, 2006, vol. 152, no. 8, pp. 2421–2431.
- Blilou, I., Xu, J., Wildwater, M., et al., The PIN Auxin Efflux Facilitator Network Controls Growth and Patterning in *Arabidopsis* Roots, *Nature*, 2005, vol. 433, pp. 39–44.
- Casimiro, I., Beeckman, T., Graham, N., et al., Dissecting *Arabidopsis* Lateral Root Development, *Trends Plant Sci.*, 2003, vol. 8, no. 4, pp. 165–171.
- Cooke, T.J., Poli, D., Sztein, A.E., et al., Evolutionary Patterns in Auxin Action, *Plant. Mol. Biol.*, 2002, vol. 49, pp. 319–338.
- Costacurta, A. and Vanderleyden, J., Synthesis of Phytohormones by Plant-Associated Bacteria, *Crit. Rev. Microbiol.*, 1995, vol. 21, no. 1, pp. 1–18.
- De Smet, I., Tetsumura, T., De Rybel, B., et al., Auxin-Dependent Regulation of Lateral Root Positioning in the Basal Meristem of *Arabidopsis*, *Development*, 2007, vol. 134, no. 4, pp. 681–690.
- Dharmasiri, N. and Estelle, M., Auxin Signaling and Regulated Protein Degradation, *Trends Plant Sci.*, 2004, vol. 9, no. 6, pp. 302–308.
- Dolan, L., Janmaat, K., Willemsen, V., et al., Cellular Organisation of the *Arabidopsis thaliana* Root, *Development*, 1993, vol. 119, no. 1, pp. 71–84.
- Fadeev, S.I., Pokrovskaya, S.A., Berezin, A.Yu., et al., *Paket programm STER dlya chislennogo issledovaniya sistem nelineynykh uravnenii i avtonomnykh sistem obshchego vida* (Software Package STER for Systemic Studies of Systems of Nonlinear Equations and Autonomic Systems of General Form), Novosibirsk: Izd-vo NGU, 1998.
- Friml, J., Vieten, A., Sauer, M., et al., Efflux-Dependent Auxin Gradients Establish the Apical-Basal Axis of *Arabidopsis*, *Nature*, 2003, vol. 426, pp. 147–153.
- Gear, C.W., The Automatic Integration of Ordinary Differential Equations, *Comm. Ass. Comput. Mach.*, 1971, vol. 14, no. 1, pp. 176–190.
- Geisler, M. and Murphy, A.S., The ABC of Auxin Transport: the Role of P-Glycoproteins in Plant Development, *FEBS Lett.*, 2006, vol. 580, no. 4, pp. 1094–1102.
- Geldner, N., Friml, J., Stierhof, Y.-D., et al., Auxin Transport Inhibitors Block PIN1 Cycling and Vesicle Trafficking, *Nature*, 2001, vol. 413, pp. 425–428.
- Jiang, K. and Feldman, J.L., Regulation of Root Apical Meristem Development, *Annu. Rev. Cell Devel. Biol.*, 2005, vol. 21, pp. 485–509.
- Kramer, E.M. and Bennett, M.J., Auxin Transport: a Field in Flux, *Trends Plant Sci.*, 2006, vol. 11, no. 8, pp. 382–386.
- Ljung, K., Hull, A.K., Celenza, J., et al., Sites and Regulation of Auxin Biosynthesis in *Arabidopsis* Roots, *Plant Cell*, 2005, vol. 17, no. 4, pp. 1090–1104.
- Paciorek, T., Zazimalova, E., Ruthardt, N., et al., Auxin Inhibits Endocytosis and Promotes Its Own Efflux from Cells, *Nature*, 2005, vol. 435, pp. 1251–1256.
- Petrasek, J., Mravec, J., Bouchard, R., et al., PIN Proteins Perform a Rate-Limiting Function in Cellular Auxin Efflux, *Science*, 2006, vol. 312, no. 5775, pp. 914–918.
- Prusty, R., Grisafi, P., and Fink, G.R., The Plant Hormone Indoleacetic Acid Induces Invasive Growth in *Saccharomyces cerevisiae*, *Proc. Natl. Acad. Sci. USA*, 2004, vol. 101, no. 12, pp. 4153–4157.
- Sabatini, S., Beis, D., Wolkenfelt, H., et al., An Auxin-Dependent Distal Organizer of Pattern and Polarity in the *Arabidopsis* Root, *Cell*, 1999, vol. 99, no. 5, pp. 463–472.
- Sauer, M., Balla, J., Luschnig, C., et al., Canalization of Auxin Flow by Aux/IAA-ARF-Dependent Feedback Regulation of PIN Polarity, *Genes Devel.*, 2006, vol. 20, no. 20, pp. 2902–2911.
- Sieberer, T., Seifert, G.J., Hauser, M.T., et al., Post-Transcriptional Control of the *Arabidopsis* Auxin Efflux Carrier EIR1 Requires AXR1, *Curr. Biol.*, 2000, vol. 10, no. 24, pp. 1595–1598.
- Swarup, R., Friml, J., Marchant, A., et al., Localization of the Auxin Permease AUX1 Suggests Two Functionally Distinct Hormone Transport Pathways Operate in the *Arabidopsis* Root Apex, *Genes Devel.*, 2001, vol. 15, no. 20, pp. 2648–2653.
- Ulmasov, T., Hagen, G., and Guilfoyle, T.J., Dimerization and DNA Binding of Auxin Response Factors, *Plant J.*, 1999, vol. 19, no. 3, pp. 309–319.
- Vieten, A., Vanneste, S., Wisniewska, J., et al., Functional Redundancy of PIN Proteins Is Accompanied by Auxin-independent Cross-Regulation of PIN Expression, *Development*, 2005, vol. 132, no. 20, pp. 4521–4531.
- Wang, J.W., Wang, L.J., Mao, Y.B., et al., Control of Root Cap Formation by MicroRNA-Targeted Auxin Response Factors in *Arabidopsis*, *Plant Cell*, 2005, vol. 17, no. 8, pp. 2204–2216.
- Woodward, A.W. and Bartel, B., Auxin: Regulation, Action, and Interaction, *Ann. Bot.*, 2005, vol. 95, no. 5, pp. 707–735.
- Xu, J., Hofhuis, H., Heidstra, R., et al., A Molecular Framework for Plant Regeneration, *Science*, 2006, vol. 311, no. 5759, pp. 385–388.